J. Plasma Fusion Res. SERIES, Vol. 8 (2009)

Alfvén Waves In Multi-Component Plasmas

Kian RAHBARNIA[1,2], Stefan ULLRICH[1], Albrecht STARK[1,2], Olaf GRULKE[1,2] and Thomas KLINGER[1,2]

[1] *MPI for Plasma Physics, EURATOM Association 17491 Greifswald, Germany*
[2] *Ernst-Moritz-Arndt-University, Greifswald, Germany*

(Received: 1 September 2008 / Accepted: 21 April 2009)

In the linear cylindrical plasma device VINETA [REF: C. Franck, Phys. Plasmas, **9**(8), 3254 (2002)] Alfvén wave (AW) dispersion relations were measured in single- (Ar, He) and multi-ion species plasmas (Ar+O, He+Ar). The comparison of theoretically calculated dispersion relations for corresponding discharge parameters shows reasonable agreement of the dispersion behavior in theory and measurements below the ion cyclotron resonance frequency. The experimentally observed Alfvén speeds for each case are consistent with the theoretically expected ones.

Keywords: Alfvén wave, dispersion relation, multi-component plasma, magnetic field fluctuation

1. Introduction

Alfvén waves (AWs) [1], low frequency electromagnetic waves with $\omega < \omega_{ci}$ the ion cyclotron resonance frequency, are basically responsible for transport processes of magnetic energy and heat in magnetized astrophysical [2,3] and laboratory plasmas [4–8]. The dispersion behavior of an AW is determined by the evolution of the parallel electron current and the perpendicular ion current. Hence the presence of multiple ion species strongly influence the dynamics of an AW, which is an important issue in investigations concerning space [9], fusion [10] and laboratory plasmas [11].

This paper discusses a simple collisionless theory for AW dispersion in single- and multi-ion species plasmas. This forms a basis for the comparison of experimental data with theoretical calculations. The experimental device VINETA and the diagnostic systems used are outlined as well.

2. Dispersion theory

A cold, current-free plasma with one or more ion species is considered. For simplicity collisional effects are neglected. The equation of motion and the total current density $\mathbf{j}$ of a multi-ion plasma with density n_k, mass m_k, velocity $\mathbf{v}_k$ and charge $q_k = Z_k e$, where k indicates the number of ion species (for electrons $Z_k = -1$), can be written as

$$m_k \frac{\partial \mathbf{v}_k}{\partial t} = q_k(\mathbf{E} + \mathbf{v}_k \times \mathbf{B}) \tag{1}$$

$$\mathbf{j} = \sum_k n_k q_k \mathbf{v}_k \,, \tag{2}$$

with the electric and magnetic field $\mathbf{E}$ and $\mathbf{B}$, respectively.

Let $\mathbf{B} = (0, 0, B_z)$, $\omega_{ci,k} = q_k B/m_k$ (ion cyclotron frequency) and $\omega_p^2 = nq^2/(\epsilon_0 m)$ (plasma frequency). We consider plane waves of the form

$$\mathbf{E} = \mathbf{E}_0 e^{i(\mathbf{k}\cdot\mathbf{r} - \omega t)} \tag{3}$$

with wave vector $\mathbf{k}$, position vector $\mathbf{r}$, time t and define the refraction index $\mathbf{n} = c\mathbf{k}/\omega$ having magnitude $n = c/v$ (c: speed of light) where $v = \omega/k$ is the phase velocity. Using Maxwell's equation $\nabla \times \mathbf{E} = i\omega\mathbf{B}$ and the Fourier transform $\nabla = i\mathbf{k}$, one obtains $\nabla \times (\nabla \times \mathbf{E}) = -\mathbf{k} \times (\mathbf{k} \times \mathbf{E}) = (\omega^2/c^2)\underline{\mathbf{K}} \cdot \mathbf{E}$ and

$$\mathbf{n} \times (\mathbf{n} \times \mathbf{E}) = -\underline{\mathbf{K}} \cdot \mathbf{E} \,. \tag{4}$$

Having $\mathbf{n}$ and $\mathbf{k}$ lie in the (x, z)-plane yields $n_y = k_y = 0$. The components of $\mathbf{n} \times (\mathbf{n} \times \mathbf{E})$ are

$$\begin{bmatrix} -n_z^2 & 0 & n_x n_z \\ 0 & -(n_x^2 + n_z^2) & 0 \\ n_x n_z & 0 & -n_x^2 \end{bmatrix} \begin{bmatrix} E_x \\ E_y \\ E_z \end{bmatrix} \tag{5}$$

and the product of the dielectric tensor $\underline{\mathbf{K}}$ and $\mathbf{E}$ is

$$\underline{\mathbf{K}} \cdot \mathbf{E} = \begin{bmatrix} K_{xx} & K_{xy} & 0 \\ K_{yx} & K_{yy} & 0 \\ 0 & 0 & K_{zz} \end{bmatrix} \begin{bmatrix} E_x \\ E_y \\ E_z \end{bmatrix} . \tag{6}$$

The solution of (4) gives the cold plasma dispersion relation [12] including finite electron mass, the Hall term in Ohm's law, the vacuum displacement current and one or more ion species. As such, the dispersion relation describes all known cold plasma wave types, including the torsional and compressional AW.

The case of two ion species is described as follows, according to R. Cross [12]. The approximations $\omega \ll \omega_{ce}$ and $v_A \ll c$ are made, with the electron cyclotron frequency ω_{ce} and the Alfvén speed v_A. Let n_1 and n_2 be the number densities of the two ion species, m_1, m_2 their masses and Z_1, Z_2 their charge numbers. Then $n_e = Z_1 n_1 + n_2 Z_2$, $x = (Z_2 n_2)/(Z_1 n_1)$, $\Omega_1 = \omega/\omega_{ci1}$, $\Omega_2 = \omega/\omega_{ci2}$, $\Omega_e = -\omega/\omega_{ce}$ with $\omega_{ci1} = Z_1 eB/m_1$, $\omega_{ci2} = Z_2 eB/m_2$ and

$$v_A^2 = \frac{B^2}{\mu_0 n_1 m_1} \,. \tag{7}$$

author's e-mail: Kian.Rahbarnia@ipp.mpg.de

Introducing the following abbreviations

$$P = -\frac{(1+x)c^2}{\Omega_e \Omega_1 v_A^2} \quad (8)$$

$$R = \frac{c^2}{\Omega_1 v_A^2}\left[(1+x) - \frac{1}{1+\Omega_1} - \frac{x}{1+\Omega_2}\right] \quad (9)$$

$$L = \frac{c^2}{\Omega_1 v_A^2}\left[-(1+x) + \frac{1}{1-\Omega_1} + \frac{x}{1-\Omega_2}\right] \quad (10)$$

$$S = \frac{R+L}{2} \quad (11)$$

$$D = \frac{R-L}{2}, \quad (12)$$

the solution of (4) reduces to

$$k_\perp^2 = \frac{F^2 - G^2}{F}, \quad (13)$$

where $F = A - k_\parallel^2$, $A = \omega^2 S/c^2$ and $G = -\omega^2 D/c^2$ [12]. Eq. (13) is quadratic in $k_\parallel^2$ with solutions

$$k_\parallel^2 = A - k_\perp^2/2 \pm [G^2 + k_\perp^4/4]^{1/2}. \quad (14)$$

The $\pm$ signs give torsional and compressional wave modes, respectively. Setting $n_1 = 0$ or $n_2 = 0$ the known solution for a single ion species plasma is recovered

$$k_\parallel^2 = \frac{\omega^2}{v_A^2(1-\Omega_1)}. \quad (15)$$

These modes are still present in a two-ion species plasma. However, the torsional wave can have two resonances $k_\parallel = \infty$, one at the lower cyclotron frequency and one at the higher cyclotron frequency. Assuming that the propagation of an AW is exactly parallel or perpendicular to $\mathbf{B}$, two special cases can be discussed. If $k_\perp = 0$ Eq. (13) yields $F = \pm G$ such that $k_\parallel^2 = A \pm G$. If $k_\parallel = 0$ Eq. (13) yields $k_\perp^2 = (A+G)(A-G)/A$. Thus for the torsional wave with propagation parallel to $\mathbf{B}$ follows

$$k_\parallel^2 = A + G = \frac{\omega^2}{c^2} L. \quad (16)$$

With (10) this dispersion relation can be written as

$$k_\parallel^2 = \frac{\omega^2}{v_{A,mult}^2} \frac{(a - b\Omega_2)}{a(1-\Omega_1)(1-\Omega_2)}, \quad (17)$$

where $a = 1 + x\omega_{ci1}/\omega_{ci2}$, $b = 1 + x$ and

$$v_{A,mult}^2 = \frac{B^2}{\mu_0(m_1 n_1 + m_2 n_2)}. \quad (18)$$

3. Experimental setup

The measurements were conducted in the linear cylindrical plasma device VINETA. The vacuum vessel (total length 4.5 m, $\varnothing = 0.4$ m) is immersed in a set of 36 coils to generate a homogeneous magnetic field up to 100 mT. The low-temperature plasmas are driven by a standard helicon antenna [13, 14] ($f = 13.56$ MHz, $P = 4$ kW pulsed) at the one end of the device. Swept Langmuir probes are used to measure densities n and electron temperatures T_e of the centrally peaked plasma ($\varnothing = 0.1$ m, working gas pressure 0.1 Pa, ionization degree 35%). Typical values are $n = 5 \cdot 10^{18}\mathrm{m}^{-3}$, $T_e = 2$ eV. The ions are cold $T_i = 0.2$ eV [15]. The ion cyclotron resonance frequencies are $f_{ci}^{Ar} = 38.8$ kHz for Ar and $f_{ci}^{He} = 388$ kHz for He. The relatively low temperatures lead to ion-neutral and ion-ion collisionalities in the range of $\nu_{in} = 2 \cdot 10^4$Hz and $\nu_{ii} = 1 \cdot 10^7$Hz, respectively. Collisional effects have been shown to effect the AW dispersion behavior, especially when the AW frequency approaches f_{ci} [16]. Since collisional effects are not included in the present framework the investigations of the AW dispersion are restricted to frequencies smaller than f_{ci}.

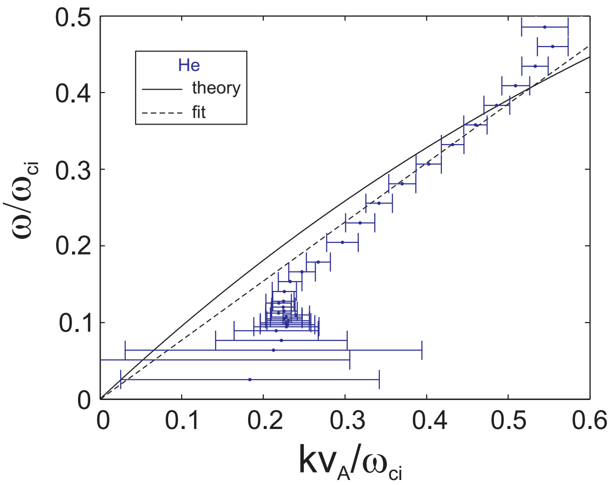

Fig. 1 Normalized AW dispersion relation in a He discharge. Also shown are the calculated dispersion relation (solid line) and a linear best fit to the measurement (dashed line).

Electromagnetic waves are excited with an insulated Helmholtz coil pair in the plasma center. Each loop has 4 windings ($\varnothing = 3.5$ cm, distance of the loops 3,5 cm). With a capacitive matching unit, typical alternating currents up to 50 A are driven, which is equivalent to a magnetic perturbation of $\tilde{B}_y \approx 5$ mT compared to $B_z = 100$ mT. Highly sensitive magnetic inductive probes are used to measure the magnetic field fluctuations of a wave. The x, y, z-loops (1000 windings each) of the probe were calibrated in a Helmholtz test field and have a lowest detection level of $B_{low} \leq 10$ nT, which is sufficiently below the expected magnetic fluctuations in the μT range. To minimize the influence on the discharge the whole probe body has been miniaturized to a length of 18 mm and a height of 10 mm, only. Great care was taken to reduce electrostatic pickup by shielding the probe.

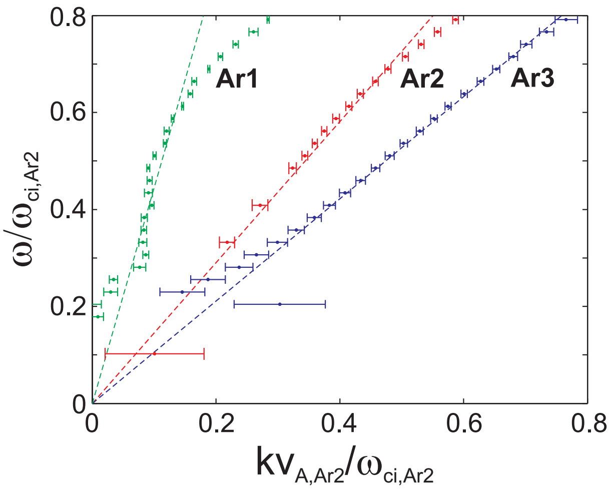

Fig. 2 Three normalized AW dispersion relations **(a)**. For [Ar1]: $B = 77\,\mathrm{mT}$, $n = 2\cdot 10^{17}\mathrm{m}^{-3}$, [Ar2]: $B = 102\,\mathrm{mT}$, $n = 5\cdot 10^{18}\mathrm{m}^{-3}$ and [Ar3]: $B = 77\,\mathrm{mT}$, $n = 4\cdot 10^{18}\mathrm{m}^{-3}$. Also shown are the linear best fits of the dispersion relations. For changing magnetic field or density the expected behavior is found.

4. Single-component plasmas

Fig. 1 shows a measured AW dispersion in a pure He discharge with $B = 102\,\mathrm{mT}$ and $n = 1\cdot 10^{18}\mathrm{m}^{-3}$ normalized to v_A and ω_{ci} of He. The calculated dispersion relation (15) (solid line) and a linear best fit to the measurement (dashed line) are depicted as well. The slope of the fit yields the Alfvén speed v_A^{fit} as listed in Tab. 1 and compared to the calculated values v_A^{calc} (7). The Alfvén speeds agree quite well, but there is a systematic deviation of $Q_A^{He} = v_A^{fit}/v_A^{calc} \approx 0.77$. In the low frequency regime fluid plasma instabilities occur [17], which strongly influence the dynamics of the AW for $kv_A/\omega_{ci} < 0.25$ and lead to fluctuations of the AW phase velocity.

Fig. 2 shows a set of measured AW dispersion relations in three different Ar discharges, where the magnetic field and the density are varied as follows: In [Ar1]: $B = 77\,\mathrm{mT}$, $n = 2\cdot 10^{17}\mathrm{m}^{-3}$, in [Ar2]: $B = 102\,\mathrm{mT}$, $n = 5\cdot 10^{18}\mathrm{m}^{-3}$ and in [Ar3]: $B = 77\,\mathrm{mT}$, $n = 4\cdot 10^{18}\mathrm{m}^{-3}$. All dispersion relations are normalized to $v_{A,Ar2}$ and $\omega_{ci,Ar2}$ of discharge [Ar2]. The Alfvén speed as obtained from the linear best fit (solid for [Ar1], dashed for [Ar2], dash-dotted for [Ar3]) can be found in Tab. 1. Here the averaged ratio is $Q_A^{Ar} \approx 1.3$.

It is concluded that the AW dispersion in single ion discharges qualitatively shows the expected behavior and reasonable agreement between the calculation and the measured Alfvén speeds is found.

The presence of an additional ion species significantly influences the propagation AWs. The investigations of AW dispersion in two-ion species plasmas follows in the next section.

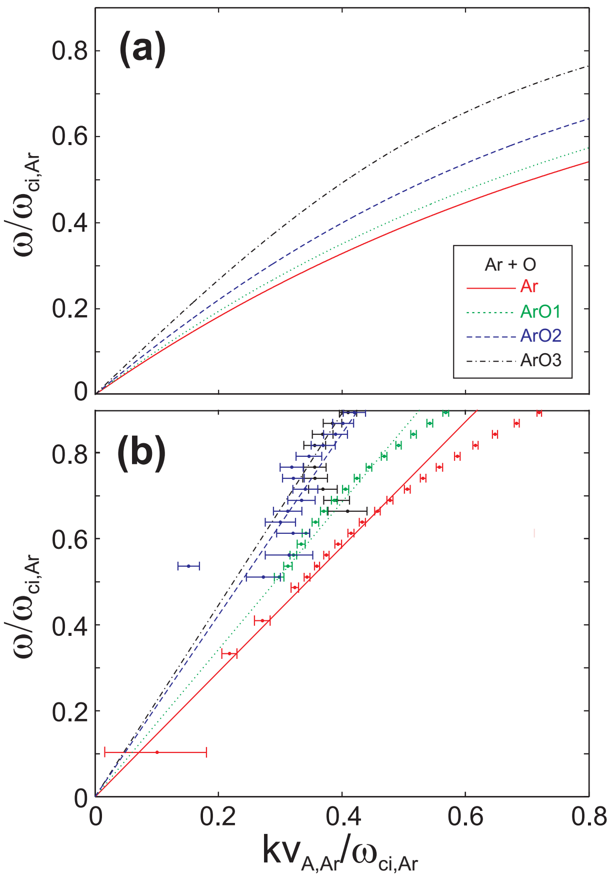

Fig. 3 Normalized AW dispersions in different mixtures of Ar and O. [ArO1] (small dash): Ar (90%), O (10%), [ArO2] (dash): Ar (55%), O (45%), [ArO3] (dash-dot): Ar (40%), O (60%) and pure Ar [Ar] (solid). (a) depicts calculated disperion relations and (b) measured dispersion relations with the corresponding linear best fits. For increasing the oxygen concentration the increasing slope of the dispersion relation can clearly be seen in theory and experiment.

discharge	v_A^{calc} $[10^5\,\mathrm{m/s}]$	v_A^{fit} $[10^5\,\mathrm{m/s}]$
Ar 1 (100 %)	5.96	7.22
Ar 2 (100 %)	1.58	2.29
Ar 3 (100 %)	1.33	1.67
He (100 %)	11	8.48
Ar (90 %) + O (10 %)	1.64	2.7
Ar (55 %) + O (45 %)	1.85	3.33
Ar (40 %) + O (60 %)	1.95	3.52

Tab. 1 Alfvén speed in different discharges (comparison of calculation and fit results). The average ratio $Q_A^{all} = v_A^{fit}/v_A^{calc}$ is 1.4.

5. Multi-component plasmas

Fig. 3 shows AW dispersion relations in a set of different mixtures of Ar and O assuming that the corresponding ratio of the partial gas pressures reflects

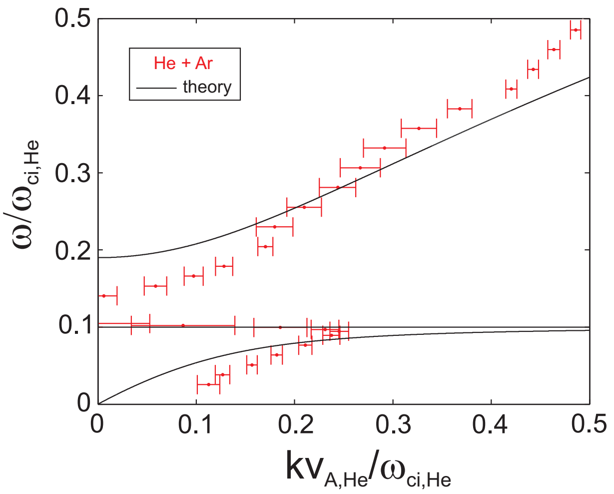

Fig. 4 Measured and calculated (solid line) AW dispersion relation in an admixture of He (90%) and Ar (10%). A good agreement of theory and experiment is observed.

the ion density ratio of Ar^+ and O^- [18]: [ArO1] (small dash): Ar (90%), O (10%), [ArO2] (dash): Ar (55%), O (45%), [ArO3] (dash-dot): Ar (40%), O (60%) and pure Ar [Ar] (solid)). Eq. (17) predicts an increase of the slope of the dispersion relation for increased concentration of oxygen as the negative ion species (Fig. 3 (a)). The calculated Alfvén speeds (18) for each case are compiled in Tab. 1. The measurements (Fig. 3 (b)) follow the expected trend. The corresponding Alfvén speeds observed in the experiment agree quite well with theory (Tab. 1, $Q_A^{mix} \approx 1.75$).

For a mixture of two positive ion species (He 90%, Ar 10%) the AW dispersion relation is shown in Fig 4. The axes are normalized by the Alfvén speed and ion cyclotron resonance frequency of the major component He. In this case (17) yields a cutoff at $0.19\,\omega_{ci,He}$ and a resonance at $0.1\,\omega_{ci,He}$, which is exactly the cyclotron resonance frequency of the minor component Ar. This resonance is also clearly seen in the experimental data (Fig 4). Above the resonance the slope of the measured dispersion relation is slightly steeper.

6. Summary

The measured AW dispersions in single- and multi-ion species helicon plasmas satisfy over a wide range of parameters (varying density, magnetic field, ion mass and mixing ratio of positive and negative ion species) the behavior of theoretically calculated dispersion relations. Except for a relatively small factor of $Q_A^{all} = v_A^{fit}/v_A^{calc} \approx 1.4$ the experimentally observed Alfvén speeds show reasonable agreement with the prediction (see Tab. 1), although the plasma collisionality is not considered.

Future studies shall focus on frequency ranges close to ω_{ci}. Detailed investigations concerning the influence of high collision frequencies and kinetic effects on the ion cyclotron resonance AWs are under way.

Acknowledgments

Konrad Sauer is gratefully acknowledged for helpful discussions concerning theoretical background of AW dispersion behavior. This work has been done in the framework of the SFB-TR24, project A1.

[1] H. Alfvén, Nature, **150**, 405 (1942)
[2] E.J. Smith et al., Adv. Space Res **20**(1), 55 (1997)
[3] D. Sundkvist, Ann. Geophys. **23**(3), 983 (2005)
[4] D. Laveder, Phys. Plasmas **9**(1), 293 (2002)
[5] F.J. Paoloni, Plasma Phys. **15**(6), 475 (1973)
[6] C. Watts, J. Hanna, Phys. Plasmas **11**(4), 1358 (2004)
[7] W. Gekelmann et al., Plasma Phys. Controll. Fusion **39**(5A), 101 (1997)
[8] G. Besson et al., Plasma Phys. Controll. Fusion **28**(9A), 1291 (1986)
[9] H. Pecseli, Solar Physics **194**, 73 (2000)
[10] G. Gnavi et al., Phys. Rev. E **54**(4), 4112 (1996)
[11] T.X. Zhang, Phys. Plasmas **11**(5), 2172 (2004)
[12] R. Cross, *An introduction to Alfvén waves*, Adam Hilger, Bristol and Philadelphia (1989)
[13] F.F. Chen, *High density plasma sources*, Noyes Publications, New Jersey (1995)
[14] R.W. Boswell, Plasma Phys. Controll. Fusion **26**(10), 1147 (1984).
[15] A. Stark et al., AIP Conf. Proc. **812**(1), 141 (2006)
[16] Y. Amagishi et al., Phys. Rev. Lett. **71**, 360 (1993)
[17] C. Schröder et al., Phys. Plasmas **12**(042103) (2005)
[18] N. Sydorenko et al., Cont. Plasma Phys. submitted (2008)